UDC 541.1 + 620.22 + 546.171.1 / 27 + 620.18

POROUS STRUCTURE OF NANO-DIMENSIONAL BORASO-GRAPHENIC POWDERS

Petrova Vera A., Garbuz Victor. V., Lobunets Tatyana F., Tomila TamaraV.

Institute for Problems of Materials Science. I. Frantsevich National Academy of Sciences of Ukraine, Krzhizhanovsky str., 3 Kyiv, 03680, Ukraine, e-mail: wpetrowa@ukr.net; Garbuz.v1950@Gmail.com

The structural features of surface of the nano-dimensional bor-azo-graphenic powders (t-BN_g) after previous washing in boiling water were researched. The results showed that after process of purifier (washing) the powder's surface of t-BN_g characterized as slit-like micro-, mesoporous (monodispersed) structure with a narrow porous distribution in the range of 3.82 - 4.17 nm. The outer surface specific area of the powders of t-BNg according to "t - method" is 28.3 m^2/g. The inner specific surface area of the mesopores is 141 m^2/g (BJH method). The residues of boron oxonitride in the form of a purified sublimate, a white powder, extracted from a washed and dried sample of t-BNg at a temperature of 540 K and a pressure of ≤ 1.0 Pa. The sublimate, according to chemical analysis and infrared spectroscopy, was identified on the assumption of the cyclic dimer of di-hydro-di-hydroxo-di-bor-ox-azole of the composition of H(OH)[(BON)$_2$](OH)H. The model of carbamide synthesis of boron nitride, as a sequence of chemical transformations of borate-carbamide precursors in a freely radical boron-pair (> B - N <), have proposed.

Key words: *surface structure, borazographene, impurity, boroxazole, dissolution*

Introduction

Natural mineral, millimeter crystals of cubic c-BN_s was named as qingsongite [1]. All other modifications of boron nitride have considered as synthetic. In practice, graphene-like, (disordered, turbostratic) boron nitride (t-BN_g) [2 – 4] is a raw material for the production of all nanoscale powders of layered and dense modifications. Graphite-like h-BN_g is forming at temperatures up to 1773K [5 – 7]. Wurtzite-like h-BN_w and sphalerite-like c-BN_s prepared by method of compression in shock wave (CSW) of h-BN_g and t-BN_g powders [7 – 9], respectively. The layered modifications of BN in the conditions of static and gradient heating at area 2003 - 3503 K and a pressure of 5 - 18 GPa leads to the aggregation of powders of h-BN_w and c-BN_s [10 – 12]. T-BN_g is a space isomer of graphene. Varieties of boron nitride derivatives are the most similar to modifications and forms of carbon [13]. BN may to form nanofibers [14], nanotubes [15, 16], nano-films of dense modifications [17], and carbo-bor-azo hetero diamond [18]. Non-oxygen samples of t-BN_g, as well as graphene-like layers on metals in nanosized semiconductor elementary devices, have obtained by thermal decomposition of toxic element-organic borohydrides or boron-chlorides with metal calcium [19, 20, 21 – 26]. Micro-dimensional powders produced from borazohydrides have used for X-rays characteristics of powders of Graphene-like t-BNg as the standard. It have two X-rays reflections only. The first of its d_{002} equal 0.3430 nm. Second plane reflection of d_{10} - 0.2503 nm [7, 19, and 20]. *It is meaning that structure of t-BN_g have physical two-dimensionality.* Graphene-like 2D boron nitride become to graphite-like 3D modification at heating from 1270K to 1470K and up to 1773 K. Its structure differs from the graphite-like 3D modification by other laws of extinction of X-ray reflections. Crystallographic space group from $P6_3$ is ordering in to $P6_3$/mmc [7].

Well-known ordering can to be observe in case of phase transition from fluorite structure to phyrochlore, from space group Fm3m to Fd3m.

As a rule, graphenic-like boron nitride is produced massively from borate acid H_3BO_3 or B_2O_3 in acid-base interaction with carbamide $(NH_2)_2CO$ in NH_3 or N_2 (H_2) atmosphere at temperatures of 1173 K and above 1273 K [27]. However, this way of synthesis a more amount of experimental information still needs have properly explained out. The problem is that t-BN_g carbamide synthesis powders differ in their composition. The ratio of the main components is not stohiometric (B / N ≠ 1). The abnormal excess of oxygen (W_O >> 1 – 10 %, by mass). The middle size of the plane (macromolecules) nanoparticles (in Coherent Scattering Area of 2D hk_{10} reflections have 1 – 3 ... 30 – 50 nm). Values of structurally interlayer parameters have d_{002} = 0.342 – 0.358 nm [28]. The issues of cleaning and studying impurities in t-BN_g are still relevant. The study of the surface structure in case of the pure powders of graphenic-like boron nitride has practically not carried out. That would be so interesting.

In recent years, the perfect porous sorbents of BN by using of other nitrogen-containing substances with more alkaline properties were obtained. Structural units of material are considered of nano plates or sheets with a thickness of not more than three graphene-like layers [29]. The material has a branched slit-like and spherical multifunctional, meso- and macro pores surface, which provides a high dynamics of sorption-desorption processes. Experimentally established sorption relation of the mass of the oil hydrophobic type pollutions to conditional mass of the sorbent is from 30/1, next 17/1 in five cycles after cleaning by burning at 870 K. Hydrophilic soluble dyes and heavy metals of electrolytic origin were up to relation of 0.5/1. Master's programs for training specialists in area of promising to use of porous BN as mobile hydrogen storage material have been developed [30]. The main advantage of the BN-based sorbents is its ability to recycle and reuse multiple times, which gives a significant advantage over another ones.

In connection with the foregoing, the surface structure of sorption materials based on graphene-like boron nitride is complex. Therefore, the investigation of the gap (slit) component of the surface structure of these materials is of some interest. The purpose of this work was to study the dimensional, volume and planar characteristics of the slot pores of nano sized powders of graphene-like boron nitride.

Certifications of the porous structure of the batch of t-BN_g powder obtained by the carbamide synthesis method in the IPM of the National Academy of Sciences of Ukraine have carried out. Incoming control, powder washing, and the nature of the impurity have established.

Experiment

To attest the samples, a complex of chemical and physical-chemical methods of integral elements chemical analysis have used [27]. Samples were pre-washed in ethanol to dissolve possible impurities of boric acid or boron oxide, as in [48]. Part of the sample has treated with boiling water for one hour in a conical flask with a reverse water cooler. The residue have filtered off, washed and dried at a temperature of 400 K to constant weight. The content of total carbon in the solid phase decreased from 0.5 to 0.3% (by mass), hydrogen - increased from 0.2 to 0.9 % (by mass), respectively.

Investigation of the porous structure of the samples was carried out using an ASAP 2000M (Accelerated Surface Area and Porosimetry System), designed to obtain isotherms of adsorption of gases (nitrogen, argon, krypton, and other non-aggressive gases) by help with of adsorption-structural static volume method. The measurement range of this method is in the range of pore sizes from 0.3 to 300 nm. In these studies, as the adsorbed gas was used nitrogen. According to the recommendations of IUPAC [32], the classification of pores is limited in size. The super micropores have x < 0.6 – 0.7 nm; micropores 0.6 – 0.7 < x < 1.5 – 1.6 nm; mesopores 1.5 – 1.6 < x < 100 – 200 nm and macro pores x > 100 – 200 nm. Characteristic or

effective pore sizes are determined in the direction of normal to the movement of molecules when they are filling. The characteristic size of the cylindrical pore is its radius, and the slit pore is the half-width of the crack. Each pore interval corresponds to certain adsorption properties. In micropores, adsorption occurs according to the mechanism of volume filling. In mesopores, by capillary condensation, where on isotherms a characteristic loop of hysteresis was observed. It is impossible to study the isotherm of macro-pores adsorption because of its proximity to the direct $P/P_0 = 1$, where P is the adsorption pressure and P_0 is the pressure of the saturated adsorption vapors. The boundaries between different classes of pores have not precisely defined, since it also depends on their form. The basis of the method lies in the ability of solids to absorb gases and vapors. Quantitatively, this ability have depicted in the form of a dependence of the volume of gas absorbed by the sample, on the partial or relative pressure of this gas at a constant temperature. That is, in the form of isotherms of adsorption - desorption. Isotherms and hysteresis loops have interpreted by types [31, 32]. It were calculated total pore volume (V_{sum}, cm^3/g) and specific surface by the method of BET (S_{BET}, m^2/g) [33 – 35]. The total volume (V_{meso}, cm^3/g) and the surface (S_{meso}, cm^2/g) of mesopores. Differential distributions porous volume and surfaces area were calculated according to BJH theory [36, 37]. Average equivalent diameter of the pores, were calculated according to the theory of BET and BJH ($D_{average}$). Volume, surface area and the distribution of the micropores in size according to the theory of Horwath-Kawazoe (HK) [38 39, 40].

The method of X-rays have used for determine the phase composition of t-BNg powders with using of DRON-2,0 diffractometer, Cu-Kα laser radiation with ASTM library. The intensity of the lines have calculated on a 100-point scale. The values of the interplanar distances d, (E) were computed from the equation:

$$2d = \lambda/\sin\theta, \quad (1)$$

where are: – interplanar distance; λ – the wavelength equal to 0,154178nm; θ – angle of reflection.

Transmission microscopy (PEM) studies were performed with help of JEM-100 CX and JEM-2100F instruments.

The structural features of the samples have studied using the IR spectroscopy (computerized complex based on Specord M80) in the region 4000 – 400 cm^{-1}. The test samples have thoroughly mixed with KBr powder in a ratio (1:300) mg. The resulting mixture compressed into clear tablets (rectangular plates in the size of ~ 5.26 mm^2.

Results and discussion

The results of X-ray diffraction investigations and element chemical analysis of samples BN indicate about of the character of nature of impurities. The presence of whose affects the value of d_{002} in this disordered (mesomorphs), isostructural phases of t-BN_g, (Table 1).

Investigation of the porous structure

The measuring range of this method was in the range of equivalent pore sizes from 0.3 to 300 nm. The nitrogen have used as the adsorbed gas. Vacuum heat treatment (degassing) the samples of the initial and washed t-BNg at a temperature of 400 K and 540 K for making isotherms of nitrogen sorption were subjected. The obtained porosity characteristics have presented in the table 2 and in Fig. 2.

Table 1. Results of elemental chemical analyses and X-ray diffraction characteristics of t-BN_g powders [28].

Name Sample t-BN_g	Elemental account of boron, nitrogen and oxygen in samples			Interplanar distance	Average diameter particle, RKR hk_{10}
	w_B±0,1 %, mass	w_N±0,1 %, mass	w_O±0,1 %, mass	d_{002}, nm	d_a, nm
I	41,2	50,1	7,1	0,358	4 – 5
II	35,2	45,6	18,7	0,342	1 – 3

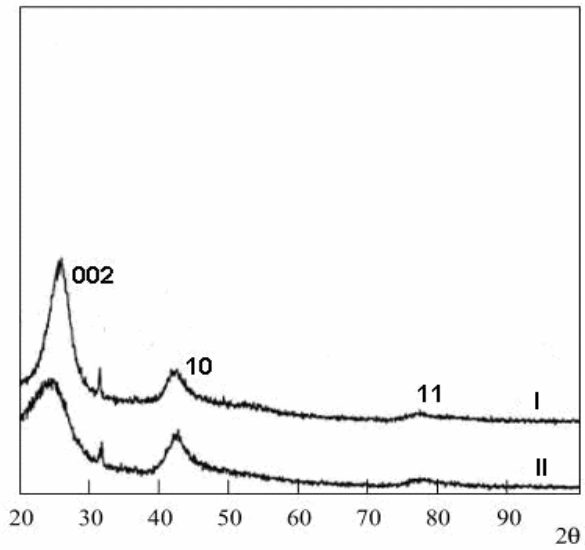

Fig. 1. X-ray diffraction of t-BN_g: I – initial sample; t-BN_g; II – washed t-BN_g [28].

Table 2. Basic porosity characteristics of samples

	Name	Sample temperature, K	V_{sum}, cm^3/g	S_{BET}, m^2/g	t-method			BJH		
					V_{micro}, cm^3/g	$S_{inner\ micro}$, m^2/g	$S_{external,\ micro}$, m^2/g	V_{meso-}, cm^3/g	S_{meso-}, m^2/g.	$D_{average}$, nm
1	I	400	$0,13_{29}$	$79,_{2}$	$0,01_{96}$	$45,_{34}$	$33,_{81}$	$0,13_{13}$	$76,_{35}$	6,9
2	I	540	$0,19_{43}$	$137,_{2}$	$0,04_{46}$	$100,_{03}$	$37,_{13}$	$0,19_{00}$	$112,_{66}$	6,8
3	II	400	$0,11_{96}$	$93,_{9}$	$0,04_{08}$	$67,_{12}$	$26,_{92}$	$0,11_{88}$	$105,_{04}$	4,5
4	II	540	$0,20_{39}$	$257,_{5}$	$0,11_{68}$	$229,_{19}$	$28,_{26}$	$0,15_{35}$	$141,_{6}$	4,3

Investigations have showed that the nitrogen adsorption isotherms of the samples refer to the IV type of classification of isotherms, which characterizes them as bodies of mesopores

(Fig. 2). The hysteresis loops of the isotherms of the investigated samples belong to the type H3. According to the classification of the hysteresis loop of isotherms, it has slit-like pores or constructed of plane-parallel particles. At the same time, desorption ledge have observed on branch of the obtained isotherms, which is characteristic for porous gaps of another structure.

The shape of the hysteresis loops of the isotherms obtained on the initial sample t-BN_g (I) is not clearly pronounced. In the sample material, in addition to the sliced pores, there are pores near to cylindrical pores (Fig. 2). At the same time, two peaks have observed in the curves of the differential distributions of the volumes and surface areas of the mesopores by size: a narrow peak in the 3 – 4nm range, which was characterized by homogeneous monodisperse bodies. Wider peaks in the range of 10 – 25 nm is typical for materials with aggregates of similar sizes. An increase of the degassing temperature for the initial sample to 540 K leads to an increasing of the sum characteristics of porosity. The degassing temperature is increasing of the volume of micropores (less than 3 nm) and some variations in the differential distributions of volume and surface area of the mesopores. The range of small pores expands, in due to at low degassing temperatures the emptying of micropores and pores with dimensions of 3 - 4 nm is partly due to the high potential of the surface. From the curves of the differential distributions of pore volumes and pore surfaces area, it follows that the initial sample has a narrow distribution in the range 3.82 – 4.17 nm (average pore diameter of 3.97_6 nm). Its number are for about 36% of the volume and 60% of the mesopores surface area. The pore in range of 10 – 25 nm are wide distributed and accounted for about 34% of the mesopores volume. The specific surface area calculated by the BET method has over estimated values. BET intended for calculating the surface of homogeneous non-porous objects whose isotherms belong to the “I” type of classification characterized for S-shaped curves. Thus, the initial powder can be presented as a micro-mesoporous body with a capillary slit structure having an internal aggregate (3.82 – 4.17 nm) and inter-aggregate (10 – 25 nm) porosity with a specific surface area of 37 m^2/g, according to the t-method, and area of the mesoporous surface have 112 m^2/g.

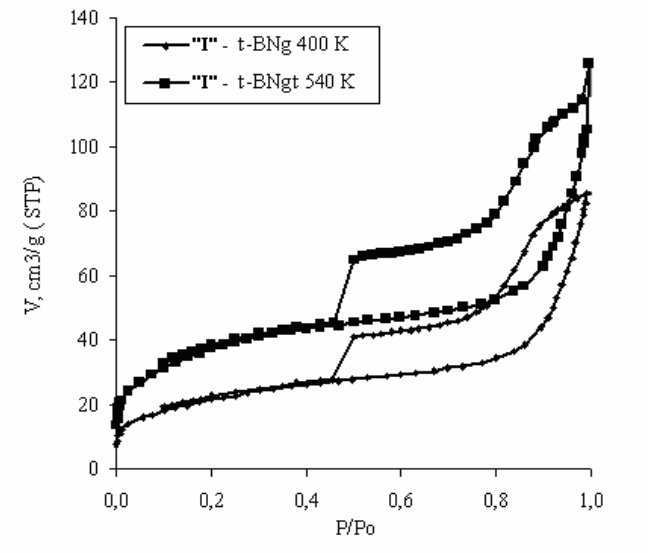

Fig.2. Isotherms of nitrogen sorption on initial samples t-BN_g.

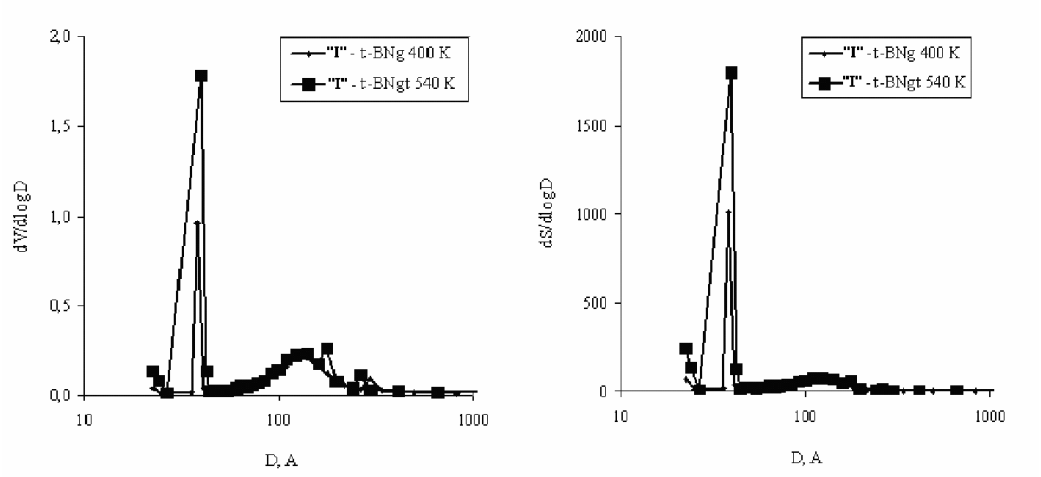

Fig.3. Differential distributions of pore volumes and surfaces area according by size of the initial t-BN_g sample.

Washing of the initial sample (II) follow to some change of its porous structure. The sorption isotherms on the washed sample t-BN_g (II) not depend from the degassing temperature. It characterize as a micro- mesopores material (Fig. 2). The hysteresis loop have become more clearly for characteristic of the slit-like pore model. An increase in temperature when degassing the treated sample to 540 K results to sublimating a white powder on the glass tube with the sample, while the color of the own sample becomes slightly creamily. The differential distributions of the mesopores volumes and surfaces are practically unchanged by size. However, the sum characteristics of the porosity substantially increase. The average size of mesopores remains the same. The number of micro- and mesopores increased. A significant increase in the specific surface area of S_{BET} is associated with the appearance of a significant volume of micropores (up to 3 nm) and is clearly overestimated. The value of the surface area calculated based on the t-method varies little. Increasing of degassing temperature promotes the release of pores of fine dimensions. Thus, an increase in the degassing temperature of a washed sample practically does not affect the porous structure of the samples, but contributes to a more complete emptying of pores of fine dimensions. Differential distributions of volumes and surfaces of mesopores by size at a degassing temperature of the sample of 540 K characterize it is as a uniformly porous (monodisperse) with a narrow pore distribution in the range 3.35 – 4.12 nm (average diameter of 3.87_6 nm), which have about 55% volume and occupies to 60% of the mesopores surface area. The range of pores over 24 nm prepare 12 – 15% of the mesopores volume (Fig. 4).

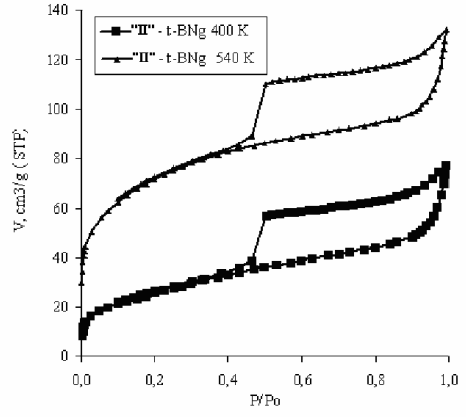

Fig.4. Isotherms of nitrogen sorption on processed samples t-BN_g.

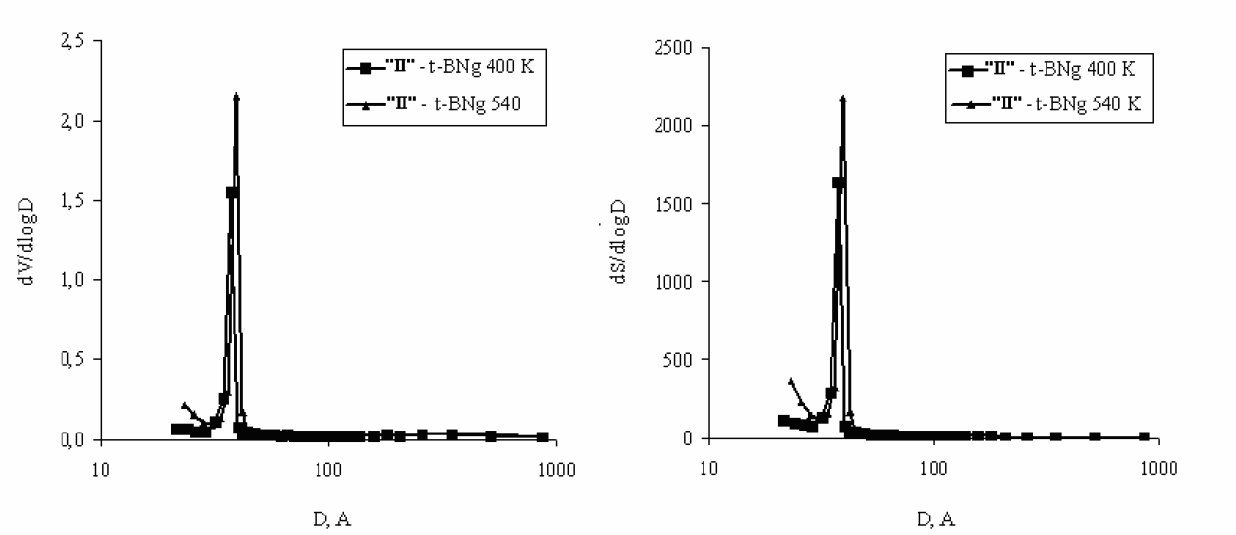

Fig.5. Differential distributions of meso-pores volumes and surfaces in sizes on processed samples t-BN_g.

To compare the porous structure of the initial and washed BN samples, the nitrogen sorption isotherms obtained at their degassing temperature of 540 K have used. The use of washing helps to obtain a more uniformly porous structure for the powder. With an almost identical total pore volume (pores with dimensions up to 300 nm), the volume of mesopores decreases, but their area significantly increases, which is a consequence of a decrease in their size. The average equivalent diameter of mesopores decreases. In addition, the volume of micropores increases. The wider distribution of mesopores on the initial sample in the 3 – 4 nm range narrows, the average mezzo-pore diameter of this range somewhat decreases - 3.87_6 nm. In this case, the porosity in the range of 10 – 25 nm practically disappears. The initial sample is converted into a mesoporous, predominantly monodisperse, slit-like structure, an essentially un aggregated material with a narrow mezzo-pore distribution by size, with the average diameter of this range decreasing from 3.97_6 nm (I) to 3.87_6 nm (II).

Thus, because of washing and vacuum-thermal treatment purification was obtained a homogeneous, micro-mesoporous, monodisperse, (with a slit-like non-rigid structure and a narrow distribution of slit-like pores in the range 3.53 – 4.12 nm), powder of graphene-like t-BN_g. The specific external surface area of the mesopores according to the t-method is ~ $28._3$ m^2/g. Specific inner surface area have 141.0 m^2/g (BJH method). Since washing (purification) of the source, material according to radiographic data leads to a decrease in the interplanar distance d_{002} from 0.358 to 0.342 nm.

Average particle diameter have calculated in the coherent scattering (RKR) region of the planar reflection hk10. According to electron diffraction data, the sizes particles from 4.0 – 5.0 nm for the initial powder decreases after washed to 1.0 - 3.0 nm. In addition, at cleaning the particle size decreases. Sublimation of cyclic dimer of boron oxonitride occurs at WTT at temperature of 540K. The poly-bor-oxonitride particles, probably, are localized in the indicated pores.

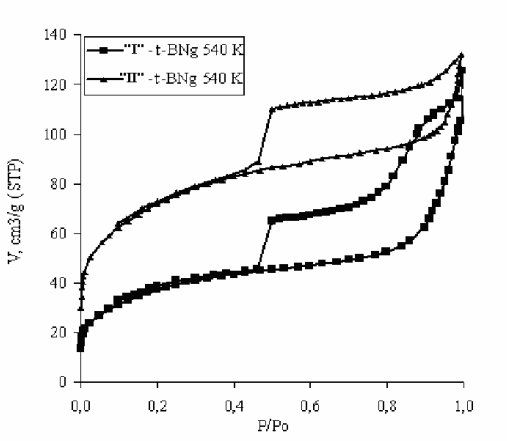

Fig. 6. Isotherms of nitrogen sorption on t-BN_g samples.

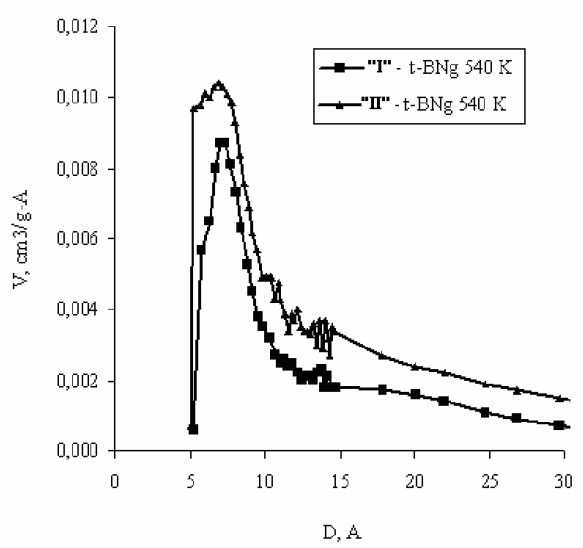

Fig.7. Differential distributions of micropores volumes by size

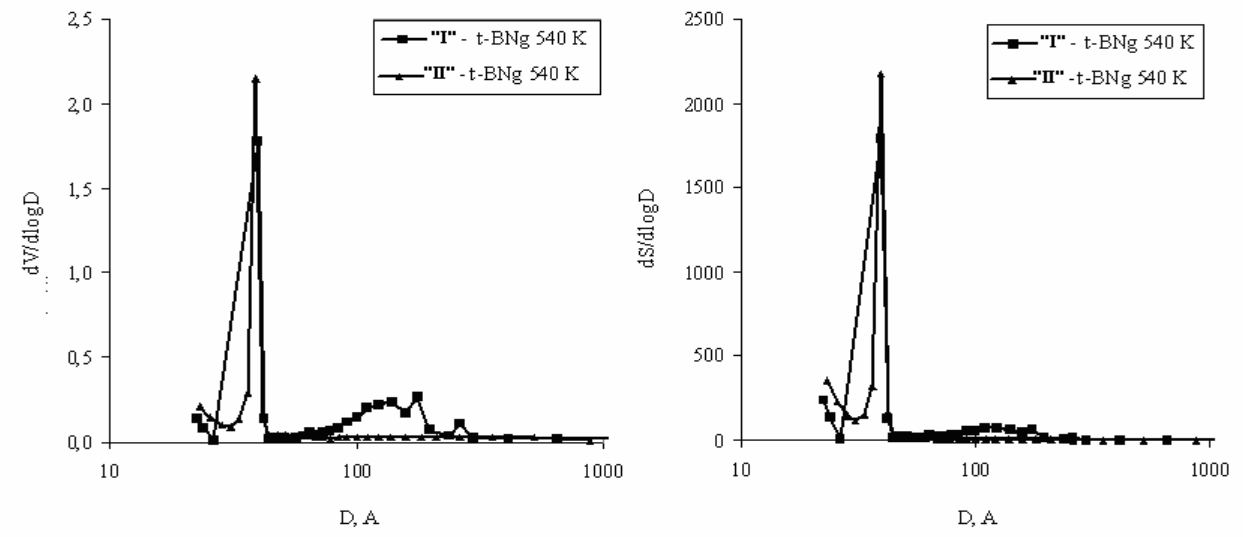

Fig.8. Differential distribution of volumes and pores surfaces by dimensions on samples t-BN_g.

The IR spectrum data of the investigated initial sample “I” have characterized by absorption bands of valence υ(BN) inner-planar and inter-planar vibrations in the region of ~ 1392 cm^{-1} and 793 cm^{-1}, respectively (Fig. 9 curve I) [28]. The arm in the frequency range ~ 1330 - 1230 cm^{-1} refers to the valence asymmetric vibrations of υ (B-O-B) in the trigonal coordination of boron [45]. The broad absorption band of the powder υ(1030 - 930) cm^{-1} and the weak absorption band in the region of ~ 464 cm^{-1} related to valence and deformation vibrations of υ(B-O-N) bonds [28, 46-48]. The absorption band with frequency of□~ 1100 cm-1 may be assigned to the planar vibrations of υ (B-O-H) [48]. In the region of ~ 3,000 - 2800 cm^{-1}, bands characteristic of valence vibrations υ (CH) appear. Hydrogen-containing vibrations of NH and OH groups are characterized by the presence of absorption bands of deformation vibrations of □ δ(NH) -1550 cm^{-1}, □ δ(OH) -1620 cm^{-1}, and valence vibrations in the frequency range □ υ(NH) ~ 3750-3300 cm^{-1}, □ υ(OH) - 3430 - 3200 cm^{-1}.

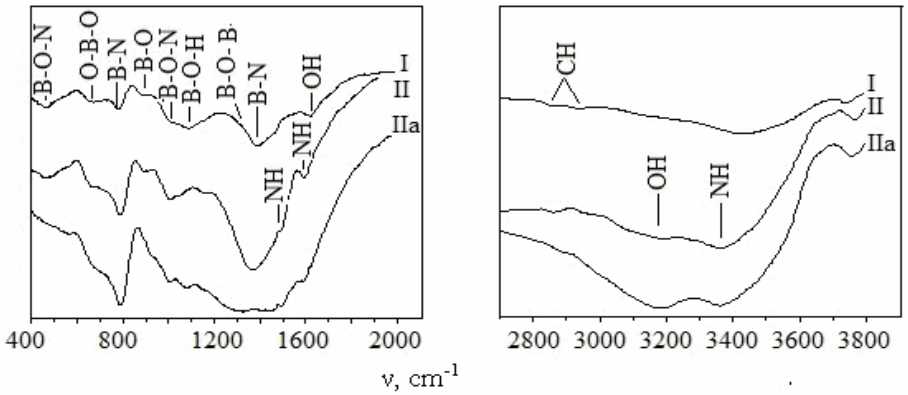

Fig. 9. IR-spectra of powders t-BNg [28]: I - starting powder; II - purified by boiling and WTT sample t-BN_g residue; IIa - sublimate.

Analysis of the IR spectrum of sample "II" t-BNg purified by the WTT (temperature 540 K) showed that the absorption bands in the region of □ ~ 1340 – 1100 cm-1, characteristic for B-O-B and B-O-H vibrations disappeared (Fig. 9, curve II). The intensity of the absorption bands characteristic of B-N, OH, and NH vibrations have increased with respect to the initial sample t-BNg. The absorption bands characterizing the vibrations of the B-O-N bond are present in the IR spectrum of the purified WTT sample of t-BNg. This indicates that the bond is so strong. It is difficult completely remove oxygen by the WTT.

The IR spectrum of sublimated powder have shown in Fig. 9. Curve IIa have characterized by wide diffuse absorption bands characteristic of a disordered amorphous structure in the region of 1900 – 900 cm^{-1}. Bands of absorption are characterized for vibrations of B–O, B–O–H, B–O–B, BN, NH and OH. Analysis of the results of IR spectroscopy suggested of powders produced by urea synthesis have provided. A complex with characteristic vibrations of B–O, B–O–N, B–O–H, B–O–B, BN, and OH bonds have formed In addition to t-BN_g. It was assumed that poly-condensed compound in the form of flat particles t-BNg formed as transition state of poly types from B_2O_3 to BN [46].

The sequence of chemical transformations in the carbamide synthesis of boron nitride is complemented by the process of stabilizing the monomers H_2N-B=O by its cyclization. In due to the fact that the interaction of borate acid with urea is the reaction of acid neutralization with the base - urea or ammonia. It is the evaluation of CO_2 from the urea residue and the multistage dehydration that ends with the formation of the final product of BN. Acid properties of the borate component in the forms of Orto-, meta-borates or anhydride lead to a series of successive reactions with the formation of the main product - nanosized particles of turbostratic-boron nitride (2).

$$2O{=}B\text{-}OH + (H_2N)_2{=}CO \rightarrow \xrightarrow{-H2O;\ -CO2} \rightarrow 2H_2N\text{-}B{=}O \rightarrow \xrightarrow{-H2O} \rightarrow {=}B\text{-}N{=} \rightarrow$$

$$\rightarrow (BN)_3 \rightarrow (BN)_{3n} \qquad (2)$$

The presence of a certain number of dissociated molecules of meta-borate acid changes the way of interaction with urea. Amino groups are exchanged with dissociated protons with the formation of formaldehyde $H_2 > C = O$ and amine meta-borate $O = B - O - NH_2$. The latter its dimerized into cyclic di-hydro-di-hydroxo-boroxazole $H(OH)[(BON)_2](OH)H$, whose dehydration enables the formation of polymeric planar particles of analogies t-BN_g, soluble in water. The sequence of transformations have represented by the following schematic sketch (3):

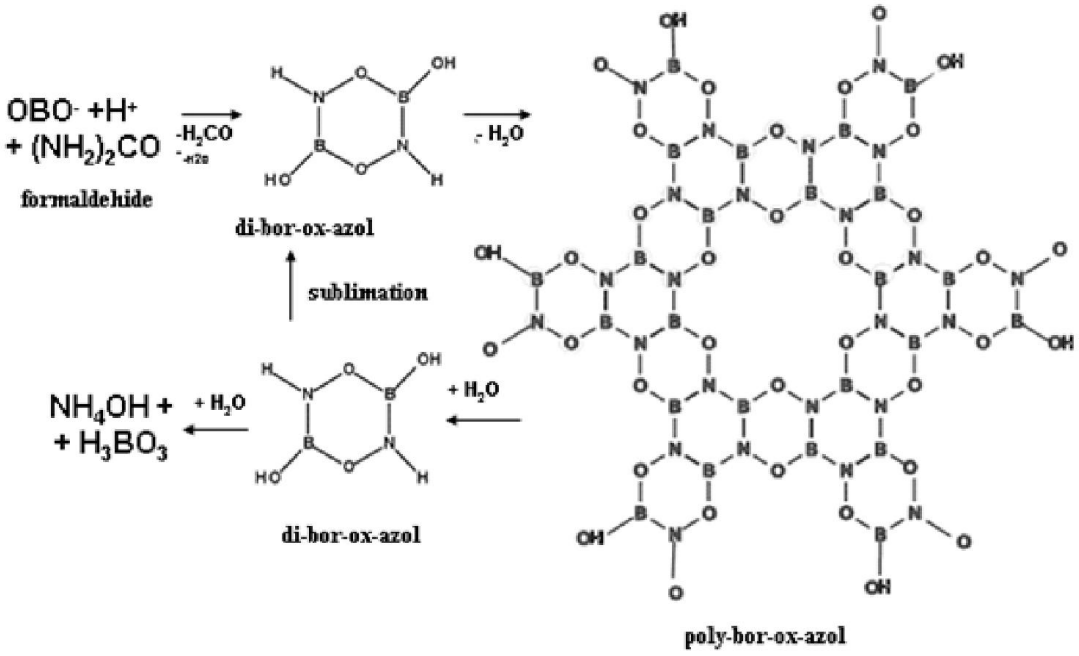

Schematic sketch (3):

Dimeric sublimate, the remnant of the disintegration of boron oxonitride polymer, was experimentally isolated with a vacuum for thermal purification of a turbostratic BN powder at a temperature of 540 K and a pressure of ~ 1.0 Pa [12]. Proceeding from the proposed reactions (2, 3), in the carbamide synthesis of boron nitride as model for the formation and stabilization of boron oxonitride in the form of a structural scetch shown in the figure 10.

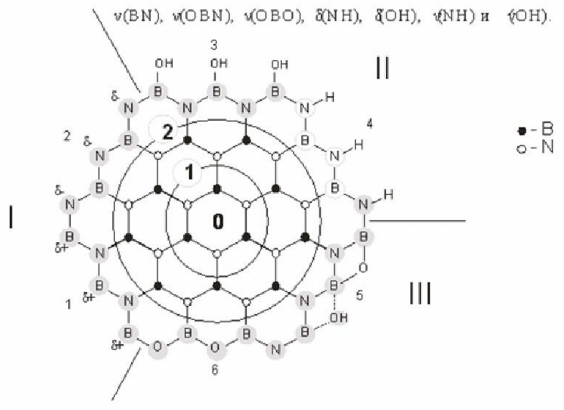

Fig. 10. Model of levels (I 1, 2 – II 3, 4 – III 5, 6) of hydrolysis of the peripheral perimeter of boron and nitrogen atoms of a macromolecules of t-BN_g. Degree of polymerization, n - 0; 1; 2. The presence of these vibrations in the IR spectra of samples indicates the coexistence of all these levels.

Segments:

I) the initial state 1 and 2 - the compensability of charges δ^+ and δ^- in peripheral atoms of B^{3+} and N^{3-};

II) 3 - joining of OH^- groups to boron $\delta^+$and 4 - the addition of H^+ to nitrogen δ^-in the interaction with water vapor in the air;

III) 5 - dehydration of neighbors OH^- groups of boron and 6 - replacement of nitrogen N^{3-} with O^{2-} - oxolation (occurrence of non-stoichiometric).

In the infrared spectra of real samples t-BN_g, there are bands of II and III levels of peripheral interaction with H_2O.

1 and 2 - in the absence of atoms and groups of joining and substitution,

3 - Hydroxylation of boron,

4 - Hydrogenation of nitrogen in contact with water vapor.

5 - Dehydration of boron,

6 - Nitrogen thermo hydrolysis, occurrence of non-stoichiometric B/N < 1.

The model indicates the presence of structural state features such as non-stoichiometric and oxygen content. It have confirmed by the results of experimental studies using chemical and chemical-phase analysis, IR spectroscopy, X-ray and electron transmission microscopy (Fig. 11).

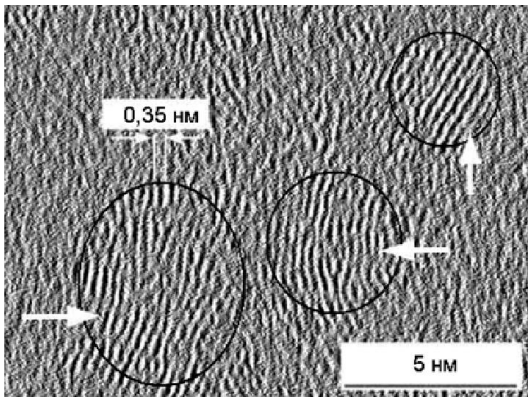

Fig. 11. Transmission electron microscopy of the t-BN_g [28].

Conclusion

The results of the work of recent years have formed a new scientific direction. Its purpose is to obtain and certify new renewable sorbents. Local and large-scale cleaning of water resources of the environment justifies the financial and intellectual costs for their creation. Powders and porous ceramic materials based on graphene-like boron nitride (BN_{graph}) with a developed external and internal surface are recognized to be a real solution to this global problem. The problem is complex. To realize the goal, it is necessary to perform a number of interrelated tasks.

These include the methods and techniques of synthesis of BN_{graph}. In the field of binary boron-azo synthesis, real success has been achieved in the use of other nitrogen-containing precursors instead of urea. Such variations are very interesting in scientific terms. However, it would be a real technological shock to solve this problem by appropriately modifying a lot of tonnage carbo-thermic synthesis of BN.

The task of studying the complex surface structure of the BN_{graph} have still not completely solved. In this paper, an attempt was made to consider only one component, a slit-like porosity, with the example of nanosized powders. Studies have shown that other materials, based on the turbostratic boron nitride, have other of pores types too.

The complexity of the pore surface structure is combined with its multifunctionality. The super-hydrophobicity of graphene-like layers causes a high sorption ability to absorb oil products from the water surface. The mechanical mobility of these layers affects the scale of variation of the interplanar distances d_{002} from 0.342 to 0.40 nm and more. Atoms of nitrogen and boron with broken chemical bonds, as a result of hydrolysis (Fig. 10), acquire the known ion-exchange properties of chemisorption of cations of heavy metals and water-soluble dyes.
The next tasks, along with high and stable sorption characteristics, are the ways of regenerating sorbents for their repeated use. The tasks have some ecological, but technological interest in the concentration and processing of secondary raw materials.
In addition, finally, the tasks of categorization, standardization of finished products and marketing pre-sales research.

Practical development of the research of a scientific direction allows solving an unexpected problem. This is the use of BN_{graph} in hydrogen storage systems. If successful, such a solution can be no more difficult than in similar acetylene-storage types.

References

1. Larissa F. Dombrzhinetskaya et.al. Qingsongit, natural cubic boron nitride: The first boron mineral from the Earth's mantle. *American Mineralogist.* 2014. 99: 764.
2. Novoselov K. S., et.al. Two-dimensional atomic crystals. *PNAS.* 2005. 102: 10451.
3. Stankovich S., et.al. Graphene-based composite materials. *Nature.* 2006. 442: 282.
4. Gaim A. K., Novoselov K. S. The rise of graphene. *Nat. Mat.*2007: *183.*
5. M. Hubacek. Synthesis of Boron Nitride from Oxide Precursors. *Archived from the original 2007. http://hubacek.jp/bn/bn.htm)*
6. Engler M. Hexagonal Boron Nitride (h-BN). Application from Metallurgy to Cosmetics. *Cfi / Ber. DKG.* 2007. 84: 25.
7. Kurdyumov A. V., Brittun V. F., Borimchuk N. I., Yarosh V. V. *Martensitic and diffusion transformations in carbon and boron nitride under impact compression*. (Kiev: Kupriyanova O. O., 2005). [in Russian]
8. T. Soma, Sawaoka A., Saito S. Characterization of wurtzite type boron nitride synthesized by shock compression. *Materials Research Bulletin.* 1974. 9*:* 755.
9. S. Rudolph. Boron Nitride: Mineral Review 2000. *American Ceramic Society Bulletin. 2000.* 79*:* 50.
10. N.H. Wentorf. Cubic from of boron nitride. *J. Chem. Phys.* 1957. 26: 956.
11. L. Vel., Demazeau G., Etourneau J. Cubic boron nitride: synthesis, physicochemical properties and application. *Materials Science and Engineering.*1991. 10: 149.
12. O. Fukunaga. Science and technology in the recent development of boron nitride materials. *J. Phys. Condens. Matter.* 2002.14: 10979.
13. Robert T. Paine, Chaitanya K. Narula. Synthetic routes to boron nitride. *Chem. Rev.* 1990. 90: 73.
14. T. S. Bartnitskaya, Ostrovskaya N. F., Ul'yanova T.M., Fenochka B.V. Preparation of boron nitride fibers with use of the hydrated cellulose. I. Decomposition of hydrated cellulose impregnated with boron-containing compounds. *Powder Metallurgy and Metal Ceramics.* 1999. 38: 152.
15. Rubio Angel, Corkill Jennifer, Cohen Marvin. Theory of graphitic boron nitride nanotubes. *Physical Review.* B49: 5081.
16. D. Goldberg, Y. Bando, C.C. Tang, C.Y. Zhi. Boron nitride nanotubes. *Adv. Mater.*19.*:* 2413.
17. P.B. Mirkarimi, McCarty K., Medlin D. Review of advances in cubic boron nitride film synthesis. *Materials Science and Engineering R Reports.* 1997. 21: 47.

18. T. Komatsu. Creation of super hard B-C-N hetero diamond using an advanced shock wave compression technology. *Journal of Materials Processing Technology.* 1999. 85: 69.
19. Kosolapova T. Ya., Andreeva TV, Bartnitskaya T.S. at. al. *Non-metallic refractory compounds.* (Moscow: Metallurgy, 1985) [in Russian].
20. *Methods of preparation, properties and application of nitrides* (Sat. Articles. Kiev: ONTI IPM of the Ukrainian Academy of Sciences, 1972) [in Russian].
21. M. Corso, Auwarter W., Muntwiller M., Tamai A., Greber T., Osterwalder J. Boron Nitride Nanomesh. *Science*. 2004. 303(5655): 217.
22. *A*. Goriachko, He Y., Knapp Marcus, Over Herbert, Corso Martina, Brugger Thomas, Berner Simon, Osterwalder Juerg et al. Self-assembly of hexagonal boron nitride nanomesh on Ru(0001*). Langmuir Lett. 2007. 23*(6): 2928.
23. O. Bank, Corso M., Matroccia D., Herger R., Willmott P., Patterson B., Osterwalder J., Vanderveen J. et al. Surface X-ray diffraction study of boron-nitride nanomesh in air. *Surf. Sci. 2007.* 601: 7.
24. Lastkovsky R., Blaha P., Schwarz K., Coriachko A. et al. Boron Nitride Nanomesh Functionality from a Corrugated Monolayer. *Angew. Chem. Ed.* 2007. 46(27): 5115.
25. R. Widmer, Berner S., Groning O., Brugger T., Osterwalder J., Greber T. Electrolutic in city STM investigation of h-BN-Nanomesh. *Electrochem. Comm.* 2007. 9: 2484.
26. "The discovery of the nanomesh for everyone." *(http://www.nanomesh.ch/history.php). Retrieved 2009-06-06.*
27. Kurdyumov A. V, Bartnitskaya T. S., Lyashenko V. I. Et al. Patterns of structure formation in the carbamide synthesis of nanocrystalline graphite-like boron nitride. *Powder Metallurgy.* 2005. **11/12***:* 88. [in Russian]
28. A. V. Kurdyumov, V. F. Britun, V. V. Garbuz, T. V. Tomila, V. V. Yarosh, V. I. Lyashenko, V. B. Zelyavsky. On impurities in nanocrystalline powders of graphite-like boron nitride and their role in the process of phase transformations under impact compression. *Nanostructural Materials Science.* 2009. **2**: 25 . [in Russian]
29. Weiwei Lei, David Portehault, Dan Liu, Si Qin & Ying Chen. Porous boron nitride nanosheets for effective water cleaning. *NATURE COMMUNICATIONS.* 2013: 1. |4:1777|DOI:10.1038/ncomms2818| **www.nature.com/naturecommunications**
30. Weng Qunhong. Porosity Engineering of Boron Nitride Materials for Hydrogen Storage Doctoral *Program in Materials Science and Engineering (University of Tsukuba). 2015.* I – *VI:3.ttp://hdl.handle.net/2241/00128908*
31. Greg S., Sing K. *Adsorption, Specific Surface, Porosity*. (Moscow: Mir. 1984). [in Russian]
32. IUPAC Manual of symbols and Terminology, Appendix 2, Pt. I, Colloid and Surface Chemistry. *Pure Appl. Chem*., 31578 (1972).
33. Brunauer S. *Adsorption of gases and vapors.* (Moscow: IL. 1948). [in Russian].
34. Poltorak O. M. *Thermodynamics in Physical Chemistry*. (Moscow.: High School. 1991). [in Russian].
35. Karnaukhov A. P. *Adsorption. Texture of dispersed and porous materials*. (Novosibirsk: Science. 1999). [In Russian].
36. Barrett E. P. et al. The determination of pore volume and area distributions in porous substances. I. Computations from nitrogen isotherms. *J. Am. Chem. Soc.* 1951. 73: 373.
37. Aligizaki Kalliopi K. *Pore Structure of Cement-Based Materials: Testing Interpretation and Requirements (Modern Concrete Technology).* (Taylor & Francis, 2005).
38. Dubinin, M. V. Surface and porosity of adsorbents. *Advances in Chemistry*. 1982 51(7): 1065. [In Russian]
39. Douglas H. Everett and John C. Powl. Adsorption in slit-like and cylindrical micropores in the henry's law region. A model for the microporosity of carbons *J. Chem. Soc., Faraday Trans.* 1976. **72**(1): 619: *DOI: 10.1039/F19767200619*

40. Horvath and Kawazoe. Method for Calculation of Effective Pore Size Distribution in Molecular Sieve Carbon. *Journal of Chemical Engineering of Japan.* 1983. **16**(6): 470.
41. Zhang, X., Lian, G., Zhang, S. J., Cui, D. L. & Wang, Q. L. Boron nitride nanocarpets: controllable synthesis and their adsorption performance to organic pollutants. *Cryst. Eng. Comm.* 2012. 14: 4670.
42. Weng, Q. H. et al. Boron nitride porous microbelts for hydrogen storage. *ACS Nano.* 2013. 7: 1558.
43. Yanming Xue, Pengcheng Dai, et. al. Template-free synthesis of boron nitride foam-like porous monoliths and their high-end applications in water purification. *J. Mater. Chem. A.* 2016. **4**: 1469. ***DOI: 10.1039/C5TA08134C***
44. Li J., Lin J., et. al. Porous boron nitride with a high surface area: hydrogen storage and water treatment. *Nanotechnology. 2013. 24(15): 155603. DOI: 10.1088/0957-4484/24/15/155603.*
45. Chandkiram Gautam, Avadhesh Kumar Yadav, Arbind Kumar Singh A Review on Infrared Spectroscopy of Borate Glasses with Effects of Different Additives *International Scholarly Research Network* 2012. **Ceramics**: 1.
46. M. Hubacek, T. Sato., T. Ishii. Coexistence of Boron Nitride and Boric Oxide. *J. Solid State Chem.* 1994. 109: 384.
47. S. Yuan, L. Zhu, M. Fan et al. Fluffy-like boron nitride spheres synthesized by epitaxial growth // *Mater. Chem. and Phys. 2008. 112: 912.*
48. Derek Peak, George W. Luther and Donald L. Sparks. ATR-FTIR spectroscopic studies of boric acid adsorption on hydrous ferric oxide. *Geochimica et Cosmochimica Acta.* 2003. 67(14): 2551.

ПОРИСТА СТРУКТУРА ПОРОШКІВ НАНОРОЗМІРНОГО БОРАЗОГРАФЕНУ

Петрова В. А., Гарбуз В. В., Лобунець Т. Ф., Томила Т.В.

Інститут проблем матеріалознавства ім. І. М. Францевича НАН України, вул. Кржижанівського, 3 Київ, 03680, Україна, e-mail: wpetrowa@ukr.net

Досліджено структурні особливості порошків нанорозмірного боразографену (t-BN_g). Результати показали, що в процесі очистки порошок t-BN_g стає мікро-, мезо-пористим (монодисперсним) з вузьким розподілом мезопори в діапазоні 3,82 – 4,12 нм, де більше половини складають об'єм і близько 60% поверхні мезопор. Площа зовнішньої поверхні порошків t-BN_g ~ 30 $м^2$ / г (t-метод), внутрішньої мезопор ~ 140 $м^2$ / г (метод BJH). Характеристики поверхні цього пористого тіла за теорією БЕТ завищені вдвічі. Залишки бору оксонітриду у вигляді очищеного сублімату, порошку білого кольору, було екстраговано з промитого та висушеного зразка t-BN_g при температурі 540 К і тиску ≤ 1,0 Па. Сублімат, згідно з даними хімічного аналізу та інфрачервоної спектроскопії, ідентифікований в припущенні циклічного димеру дигідро-дигідроксо-ди бороксазолу складу $H(OH)[(BON)_2](OH)H$. Запропоновано модель карбамідного синтезу нітриду бору, як послідовність хімічних перетворень борато-карбамідних прекурсорів у вільно радикальні боразо-пари (> B – N <).

ПОРИСТАЯ СТРУКТУРА ПОРОШКОВ НАНОРАЗМЕРНОГО БОРАЗОГРАФЕНА

Институт проблем материаловедения им. И.Н.Францевича НАН Украины ул. Кржижановского, 3 Киев, 03680, Украина, e-mail: wpetrowa@ukr.net

Исследованы структурные особенности порошков наноразмерного боразографену (t-BNg.). Результаты показали, что в процессе очистки порошок t-BNg становится микро-, мезопористым (монодисперсным) с узким распределением мезопоры в диапазоне 3,82 - 4,12 нм, где более половины составляют объем и около 60% поверхности мезопор. Площадь внешней поверхности порошков t-BN_g ~ 30 $м^2$ / г (t-метод), внутренней мезопор ~ 140 $м^2$ / г (метод BJH). Характеристики поверхности этого пористого тела по теории БЭТ завышены вдвое. Остатки оксонитрида бора в виде очищенного сублимата, порошка белого цвета, было экстрагировано из промытого и высушенного образца t-BN_g при температуре 540 К и давлении ≤ 1,0 Па. Сублимат, согласно данным химического анализа и инфракрасной спектроскопии, идентифицирован в предположении циклического димера ди-гидро-ди-гидр-оксо-ди-бор-окс-азола состава $H(OH)[(BON)_2](OH)H$. Предложена модель карбамидного синтеза нитрида бора, как последовательность химических превращений борат-карбамидных прекурсоров в свободно радикальные боразо-пары (> B - N <).